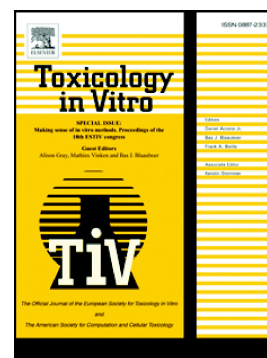


Accepted Manuscript

Synthesis and antimetastatic activity evaluation of cinnamic acid derivatives containing 1,2,3-triazolic portions

Graziela Domingues de Almeida Lima, Michelle Peixoto Rodrigues, Tiago Antônio de Oliveira Mendes, Gabriela Alves Moreira, Raoni Pais Siqueira, Adalberto Manoel da Silva, Boniek Gontijo Vaz, Juliana Lopes Rangel Fietto, Gustavo Costa Bressan, Mariana Machado-Neves, Róbson Ricardo Teixeira



PII: S0887-2333(18)30387-4
DOI: doi:[10.1016/j.tiv.2018.07.015](https://doi.org/10.1016/j.tiv.2018.07.015)
Reference: TIV 4335
To appear in: *Toxicology in Vitro*
Received date: 2 April 2018
Revised date: 25 June 2018
Accepted date: 20 July 2018

Please cite this article as: Graziela Domingues de Almeida Lima, Michelle Peixoto Rodrigues, Tiago Antônio de Oliveira Mendes, Gabriela Alves Moreira, Raoni Pais Siqueira, Adalberto Manoel da Silva, Boniek Gontijo Vaz, Juliana Lopes Rangel Fietto, Gustavo Costa Bressan, Mariana Machado-Neves, Róbson Ricardo Teixeira , Synthesis and antimetastatic activity evaluation of cinnamic acid derivatives containing 1,2,3-triazolic portions. *Tiv* (2018), doi:[10.1016/j.tiv.2018.07.015](https://doi.org/10.1016/j.tiv.2018.07.015)

This is a PDF file of an unedited manuscript that has been accepted for publication. As a service to our customers we are providing this early version of the manuscript. The manuscript will undergo copyediting, typesetting, and review of the resulting proof before it is published in its final form. Please note that during the production process errors may be discovered which could affect the content, and all legal disclaimers that apply to the journal pertain.

**Synthesis and antimetastatic activity evaluation of cinnamic acid derivatives
containing 1,2,3-triazolic portions**

Graziela Domingues de Almeida Lima^{a§}, Michelle Peixoto Rodrigues^{b§}, Tiago Antônio de Oliveira Mendes^c, Gabriela Alves Moreira^c, Raoni Pais Siqueira^c, Adalberto Manoel da Silva^d, Boniek Gontijo Vaz^e, Juliana Lopes Rangel Fietto^c, Gustavo Costa Bressan^{c*},
Mariana Machado-Neves^{a*}, Róbson Ricardo Teixeira^{b*}

^aDepartamento de Biologia Geral, Universidade Federal de Viçosa, Viçosa, Minas Gerais, Brazil

^bDepartamento de Química, Universidade Federal de Viçosa, Viçosa, Minas Gerais, Brazil

^cDepartamento de Bioquímica e Biologia Molecular, Universidade Federal de Viçosa, Viçosa, Minas Gerais, Brazil

^dInstituto Federal de Educação, Ciência e Tecnologia Catarinense, Araquari, Santa Catarina, Brazil

^eInstituto de Química, Universidade Federal de Goiás, Goiânia, Brazil

§These authors contributed equally to this work

*Corresponding authors

E-mail addresses: gustavo.bressan@ufv.br (Gustavo Costa Bressan);
mariana.mneves@ufv.br (Mariana Machado-Neves); robsonr.teixeira@ufv.br (Róbson Ricardo Teixeira).

ABSTRACT

It is herein described the preparation and evaluation of antimetastatic activity of twenty-six cinnamic acid derivatives containing 1,2,3-triazolic portions. The compounds were prepared using as the key step the Copper(I)-catalyzed azide (A)-alkyne (A) cycloaddition (C) (CuAAC reaction), also known as click reaction, between alkynylated cinnamic acid derivatives and different benzyl azides. The reactions were carried in $\text{CH}_2\text{Cl}_2/\text{H}_2\text{O}$ (1:1 v/v) at room temperature, and the triazole derivatives were obtained in yields ranging from 73%–99%. Reaction times varied from 5 to 40 min. The identity of the synthesized compounds was confirmed by IR and NMR (^1H and ^{13}C) spectroscopic techniques. They were then submitted to *in vitro* bioassays to investigate how they act over metastatic behavior of murine melanoma. The most potent compound, namely 3-(1-benzyl-1*H*-1,2,3-triazol-4-yl)propyl cinnamate (**9a**), showed significant antimetastatic and antiproliferative activities against B16-F10 cells. In addition, gelatin zymography and molecular docking analyses pointed to the fact that this compound has potential to interact with matrix metalloproteinase 9 (MMP-9) and MMP-2, which are directly involved in melanoma progression. Therefore, these findings suggest that cinnamic acid derivatives containing 1,2,3-triazolic portions may have potential for development of novel candidates for controlling malignant metastatic melanoma.

Keywords: cinnamic acid, 1,2,3-triazoles, antimetastatic, melanoma, click chemistry, gelatinases, matrix metalloproteinase, virtual molecular docking

1. Introduction

Malignant melanoma is an extremely aggressive and metastatic cancer presenting the highest rate of mortality among skin cancers. In fact, less than 10% of patients with metastatic melanoma survive up to 10 years after the diagnosis (Bathia et al., 2009). Malignant melanoma can be cured by surgical intervention in its early stages, but this approach is practically inefficient in its metastatic stage (Gray-Schopfer et al., 2007; Elias et al., 2010). In this case, treatment is extremely difficult due to the metastatic melanoma resistance to existing therapies. This resistance is related to the complex cell signaling pathways modulating the proliferation and ability of tumor cells to escape from apoptotic processes during metastasis (Gray-Schopfer et al., 2007; Hanahan and Weinberg, 2011; Siegel et al., 2015; Agaësse et al., 2017). As the process of tumor cells dissemination involves several events until the establishment of a secondary tumor site, such as cellular detachment, migration, invasion, and adhesion, as well as cell colonization and growth, these steps represent important therapeutic targets (Kumar and Weaver, 2009; Guan, 2015). Hence, there is an urgent need to discover new therapies for improving the current therapeutic strategies and, consequently, the survival of cancer patients (Elias et al., 2010).

Natural products have been explored as a source of compounds for drug discovery. Between 1981 and 2002, about 60% of the new drugs developed for cancer treatments were derived from natural products (Gullo et al., 2006; Lam, 2007; Harvey, 2008; Schmidt et al., 2008; Dias et al., 2012). Compounds currently used in clinical cancer chemotherapy, such as paclitaxel, etoposide, teniposide, and camptothecin are examples of drugs based on the natural product pool (Ali et al., 2014).

The cinnamic acid (Fig. 1) consists of an aromatic acid found in several higher plants. Typically, it occurs in nature in *trans*-geometry, and belongs to a class of plant hormones regulating cell growth and differentiation known as auxins. This acid and its

derivatives play an important role as intermediates in the production of other important compounds, such as styrenes and stilbenes (Sharma et al., 2011). It has been demonstrated that cinnamic acid derivatives display several activities including antifungal, antibacterial, and anti-inflammatory (Chiriac et al., 2005).

The antimetastatic effect of cinnamic acid derivatives against tumor cell lines has also been demonstrated (Yen et al., 2011; Tsai et al., 2013; Ling et al., 2015). For instance, *trans* and *cis* forms of cinnamic acid exhibited anti-migratory activity against human lung adenocarcinoma cells (Yen et al., 2011). A farnesyl thiosalicylic acid (FTS)-diamine/cinnamic acid hybrid (**1**, Fig. 1) also showed significant anti-migratory activity against colon carcinoma cells (Ling et al., 2015). Moreover, other derivatives of cinnamic acid, such as caffeic acid (**2**), ferulic acid (**3**) and chlorogenic acid (**4**), were capable of inhibiting the invasive behavior of human lung adenocarcinoma cells (Tsai et al., 2013).

In this framework, we describe herein the synthesis of cinnamic acid derivatives containing 1,2,3-triazolic portions. The Copper(I)-catalyzed azide (A)-alkyne (A) cycloaddition (C) (CuAAC reaction), also known as click reaction, between cinnamates having terminal triple bonds and different benzyl azides corresponded to the key step of the synthetic route designed to obtain the twenty-six cinnamic acid derivatives containing triazolic portions. Additionally, the antimetastatic activity of the derivatives was screened against B16-F10 melanoma cell line. For that, the effects on cell proliferation and colony formation were assessed using the most efficient compound found in this study. Finally, gelatin zymography analyzes pointed to the fact that this compound has the potential to reduce the matrix metalloproteinases (MMP) -9 and -2 activities, and the docking studies demonstrated that this compound have good score and docking affinity with these enzymes.

2. Materials and methods

2.1. Reagents and synthetic procedures

Solvents were purchased from Vetec (Rio de Janeiro, Brazil). Commercially available pent-4-yn-1-ol, prop-2-yn-1-ol, benzyl alcohols, triethyl amine, dimethyl sulfoxide (DMSO), *N,N'*-dicyclohexylcarbodiimide (DCC), 4-*N,N'*-dimethylaminopyridine (DMAP), sodium ascorbate, sodium azide and copper(II) sulfate pentahydrate were purchased from Sigma Aldrich (St. Louis, MO, USA) and used without further purification. Details concerning the preparation of the compounds investigated herein can be found in the supplementary material.

2.2. Biological evaluation

2.2.1. Cell culture and culture conditions

Metastatic melanoma cells (B16-F10) were kindly provided by Dr. Anésia Aparecida dos Santos (Department of General Biology, Universidade Federal de Viçosa (UFV), Viçosa, Minas Gerais, Brazil). Embryonic fibroblasts cell line (NIH3T3) was kindly provided by Dr. Leandro Licursi de Oliveira (Department of General Biology, UFV, Viçosa, Minas Gerais, Brazil). The African green monkey kidney cell line (Vero) was kindly provided by Dr. Juliana Lopes Rangel Fietto (Department of Biochemistry and Molecular Biology, UFV, Viçosa, Minas Gerais, Brazil). Cell lines were grown in RPMI-1640 medium (Sigma) supplemented with 10% (v/v) fetal bovine serum (FBS; LGC Biotecnologia, São Paulo, Brazil), 100 $\mu\text{g mL}^{-1}$ of streptomycin, and 100 units mL^{-1} of penicillin (Sigma) at pH 7.2 and 37 °C under 5% CO_2 atmosphere.

2.2.2. Cell viability assay

Cell viability was determined with the MTT ((3-(4,5 dimethylthiazol-2-yl)-2,5 diphenyltetrazolium bromide; Sigma). B16-F10 cells were seeded onto 96-well plates at a concentration of 1×10^4 cells/well. Each well contained 100 μL of complete RPMI

medium and 100 μL of each compound solution at different concentrations (0-200 $\mu\text{mol L}^{-1}$). The compounds **8a–8m** and **9a–9m** were diluted in RPMI medium with 10% FBS plus 0.4% v/v DMSO (Sigma). After 48 h of culture, MTT (5 mg mL^{-1} ; Sigma) was added to each well, and incubated for 4 h at 37 °C. The MTT solution was then removed, and DMSO at 100 μL /well was added to solubilize the formazan. Absorbance was measured at 540 nm in a microplate reader (SpectraMax M5, Molecular Devices, California, USA). Results were normalized considering the cultures treated with 0.4% DMSO (control), and the half-maximal inhibitory concentration (IC_{50}) was calculated according to Siqueira et al. (2015).

2.2.3. Cell migration assay

The wound-healing assay is a method widely used to study directional cell migration *in vitro*, which mimics cell migration during wound healing *in vivo* (Rodrigues et al., 2005). Thus, it was conducted to evaluate the ability of cinnamic acid derivatives to inhibit cell migration, based on a previous published methodology (Liang et al., 2007; Anasamy et al., 2017) with modifications. B16-F10 cells were seeded onto 24-well plate at a concentration of 2×10^5 cells/well, and allowed to reach full confluence after incubation overnight at 37 °C under 5% CO_2 atmosphere. Monolayers were then wounded using a sterile 200 μL pipette tip. Cells were washed twice with phosphate buffered saline (PBS) to remove detached cells, and then treated with compounds **8a–8m** and **9a–9m** at the concentration of 100 $\mu\text{mol L}^{-1}$. The compounds with inhibitory effect on cell migration were tested at the concentration of 50 $\mu\text{mol L}^{-1}$. DMSO (0.4% v/v) was used as control. Photos of the wound were taken using an inverted microscope (EVOS fl, Life Technologies, Canada). Wound closure rates were then calculated quantitatively as the difference between wound width at 0 and 24 h. Results were expressed as percentage of cell migration.

2.2.4. Cell proliferation assay

B16-F10 cells were seeded onto 6-well plates at a concentration of 1×10^5 cells/well in the presence of $100 \mu\text{mol L}^{-1}$ compound **9a**. Additionally, untreated cells were used as control using DMSO (0.4% v/v). The effect of the compound on cell growth was evaluated by trypan blue (Invitrogen, São Paulo, Brazil) dye exclusion. After 24, 48, and 72 h, cells were loaded on a hemocytometer to obtain the viable cell count (Pietraszek et al., 2013).

2.2.5. Cell invasion assay

This assay was carried out using transwell inserts with pore diameter of $8 \mu\text{m}$ (Millicell, Ireland) based on protocols previously described (Chen, 2005; Hulkower and Herber, 2011) with modifications. Briefly, $60 \mu\text{L}$ of matrigel (BD Biosciences) diluted in serum free medium (1:12) was added to the upper chambers, and incubated for 1 h at $37 \text{ }^\circ\text{C}$ to gel formation. Thereafter, B16-F10 cells at 1×10^5 cells/well were diluted in serum free medium and treated with compound **9a** at different concentrations (12.50, 25 and $50 \mu\text{mol L}^{-1}$) for 1 h. Cells were then seeded onto the upper surface, whereas a medium containing 10% FBS was added in the lower surface. After 24 h of incubation, filter inserts were removed from the wells. The cells on the upper surface of the filter were wiped with a cotton swab. The cells that invaded the lower surface were fixed with methanol for 10 min, stained with 0.5% toluidine blue solution (Sigma), and then counted under a microscope using ten randomly chosen fields/ group. DMSO-vehicle treatment at 0.4% (v/v) was used as control. Results were expressed as percentage of cell migration.

2.2.6. Cell-matrix adhesion assay

After treatment with 12.50, 25 and $50 \mu\text{mol L}^{-1}$ of compound **9a** for 30 min, the cells (5×10^4 cells/well) were seeded onto 96-well matrigel-coated plates, and incubated

overnight at 37 °C under 5% CO₂ atmosphere. Non-adherent cells were removed by gentle washing with PBS. The adherent cells on the plate were measured by MTT assay.

2.2.7. Clonogenic assay

For clonogenic assay, B16-F10 melanoma cells (1000 cells per well) were seeded onto a 6-well plate and incubated overnight at 37 °C under 5% CO₂ atmosphere. Subsequently, exhausted medium was changed with fresh medium containing 12.50, 25 and 50 μmol L⁻¹ of compound **9a**. Culture treatment was carried out for 24 h and the cells were cultured for 14 days with growth medium replaced at every two days. On the 15th d, colonies were fixed with methanol, stained with 0.5% toluidine blue solution, and finally counted (Mao et al., 2016). Results were expressed as percentage of untreated control cultures.

2.2.8. Cytotoxicity on non-tumor cell lines

The cytotoxicity of compound **9a** was tested on two non-tumor cell lines. Cell NIH3T3 (1x10⁴ cells/well) and Vero (3x10⁴ cells/well) were seeded onto 96-well plates, and cell viability was determined by MTT assay previously described (Pietraszek et al., 2013).

2.2.9. Hemolysis assay

This assay was used to determine the compatibility of erythrocytes to compound **9a**. Blood was collected from a five healthy C57BL/6J male mice, centrifuged at 700 g for 10 min, washed three times with 0.9% saline solution (m/v), and resuspended in the same buffer to prepare 2% red blood cell suspension (Xu et al., 2017). Subsequently, different concentrations (0–100 μmol L⁻¹) of the compound **9a** were incubated with the suspension at 37 °C. The red blood cells were also incubated with saline solution (0.9% m/v) and triton (1% v/v) as negative and positive control, respectively. After 2 h, the samples were centrifuged for 10 min at 700 g and it was determined the release of

hemoglobin by photometric analysis at 540 nm. The described procedures above are in agreement with the ethical principles of animal research adopted by the Animal Ethics Committees (CEUA protocol number 27/2015).

2.2.10. Predicting ADMET properties of **9a**

In order to predict ADMET (Absorption, distribution, metabolism, excretion, toxicity) properties of compound **9a**, it was utilized the pkCSM approach which uses graph-based signatures to develop predictive models of central ADMET properties for drug development (Pires et al., 2015). Herein, it was evaluated the *in silico* ADMET characteristics of compound **9a** using the freely accessible web server <http://biosig.unimelb.edu.au/pkcsm/prediction> and the SMILES O=C(OCCCC1=CN(CC2=CC=CC=C2)N=N1)\C=C\C1=CC=CC=C1 related to compound **9a**.

2.2.11. Gelatin zymography

B16-F10 cells were incubated with 50, 100 and 150 $\mu\text{mol L}^{-1}$ compound **9a** for 24 h. The media were then collected and centrifuged at 1,500 rpm for 6 min at 4 °C to remove cells debris. The cell-free supernatant was mixed with a 4X non reducing sample buffer and electrophoresis was performed using precast gel (10% polyacrylamide and 0.1% gelatin as a protease substrate). Following electrophoresis, the gel was washed twice in 2.5% Triton X-100 for 1 h to remove sodium dodecyl sulfate (SDS), subsequently washed in an activation buffer containing CaCl_2 and incubated in this buffer at 37 °C for 18 h. The gel was, then, stained with Coomassie blue R-250 (0.125% Coomassie blue R-250, 50% methanol, and 10% acetic acid) followed by destaining (methanol/acetic acid/water, 40/10/50, v/v) (Lee et al., 2015). The protein content was determined according to the method described by Bradford using BSA as a standard (Bradford, 1976).

2.2.12. Computational simulation of the interaction between compound **9a** and MMP-9 and -2

Molecular docking analyses of the synthesized compounds **8a–8m** and **9a–9m** were simulated to determine the relative affinity with MMP-9 and MMP-2 enzymes using AutoDock Vina release 1.1.2 (Trott and Olson, 2010). The crystal structure of MMP-9 (PDB ID: 1L6J) and MMP-2 (PDB ID: 1QIB) was extracted from Protein Data Bank. The activity site of enzymes was identified by selection of amino acids within 12 Å radius from zinc ions that participate of the catalytic mechanism. The 3D structures of all compounds were drawn, optimized and protonate using MarvinSketch software (Chemaxon®). Binding energy was estimated using Auto Docking Tools implemented in PyRx plataform. Docked structures were visualized and edited using PyMOL software.

2.3. Statistical Analysis

All numeric data were done in three independent replicates. The values were expressed as mean \pm standard error mean (S.E.M). Statistical analyses were performed using Microsoft Excel (Microsoft Office Software), and GraphPad Prism (GraphPad Software Inc.). Statistical analyses were submitted to one-way ANOVA followed by Dunnett's test.

3. Results and discussion

3.1. Synthesis

The synthesis of cinnamic acid derivatives containing triazolic portions required the preparation of esters **5** and **6**, as well as a series of azides **7** (Fig. 2). Thus, the Steglich esterification (Sova et al., 2006) between *trans*-cinnamic acid and different alcohols afforded compounds **5** and **6** in good yields (68% and 83%, respectively) after purification by silica gel column chromatography. Azides **7** were prepared from the

corresponding benzylic alcohols (Fig. 2) using a methodology previously described (Borgati et al., 2013).

The click reaction between esters **5** and **6** and azides **7** (Fig. 3) afforded the desired cinnamic acid derivatives **8a–8m** and **9a–9m** in yields ranging from 73% to 99%. Further details concerning the structures of the synthesized compounds and characterization of them can be found in the supplementary material.

It should be mentioned that the synthesis of these compounds was planned in order to evaluate the influence of different benzyl groups (attached to the triazole ring), as well as the size of the aliphatic carbon chain (connecting the cinnamic acid portion and the triazole functionality) on biological responses.

3.2. Cinnamic acid derivatives reduce metastatic potential of B16-F10 cells

Migration is an important step in cancer metastasis, and cancer cells have a strong migration behavior (Shtivelman et al., 2006; Astin et al., 2010). In order to examine the effect of the synthesized compounds **8a–8m** and **9a–9m** on B16-F10 cell migration, we performed wound-healing assays in the presence of compounds to evaluate the cell motility. In this assay, we used the concentration of $100 \mu\text{mol L}^{-1}$ considering that all compounds had low cytotoxicity based on IC_{50} (data not shown). Nineteen of the twenty-six derivatives synthesized significantly suppressed B16-F10 cell migration at $100 \mu\text{mol L}^{-1}$ (**8a**, **8b**, **8f**, **8h**, **8i**, **8j**, **8l**, **8m**, **9a**, **9b**, **9c**, **9d**, **9e**, **9g**, **9h**, **9i**, **9k**, **9l** and **9m**) compared to vehicle-treated cells (0.4% DMSO) (Fig. 4A and B). Moreover, compounds **8a**, **8b**, **8l**, **8m**, **9a**, **9c**, **9e**, **9h**, **9l** and **9m** were the most active in suppressing B16-F10 cell migration in at least 50% compared to control. Thereafter, it was evaluated the anti-migratory efficacy of these ten most effective derivatives at $50 \mu\text{mol L}^{-1}$ (Fig. 4C). In this case, only compound **9a** significantly suppressed the cell

migration in approximately 86% ($p \leq 0.0001$) in comparison with the control (Fig. 4D). Therefore, compound **9a** (Fig. 4E) was chosen for further experiments.

In addition to migration, B16-F10 cells may close the scratch by cell proliferation. Based on that, we also evaluated the effect of compound **9a** on the proliferative activity. Our findings revealed that compound **9a** significantly impaired B16-F10 cell proliferation at $100 \mu\text{mol L}^{-1}$ in a time-dependent manner (Fig. 4F). Taking these findings together, we may suggest that the compound **9a** was able to suppress cell migration and proliferation.

Invasion and cell adhesion are also key steps in melanoma metastasis. Thus, the development of compounds with anti-invasive and anti-adhesive properties is of potential interest (Shtivelman et al., 2006). Herein, we also evaluated the effect of compound **9a** on the invasion and adhesion of metastatic B16-F10 cells. B16-F10 cell invasion decreased after 24 h of treatment with compound **9a** at 12.5 (52.3%), 25 (64.2%) and 50 (76%) $\mu\text{mol L}^{-1}$ compared to vehicle-treated cells (0.4% DMSO) (Fig. 5A and B). Similarly, cell adhesion was significantly decreased at 25 (8.6%) and 50 (32.2%) $\mu\text{mol L}^{-1}$ (Fig. 5C). This remarkable activity of compound **9a** over the metastatic behavior of melanoma is in agreement with other studies that previously reported antimetastatic activity for cinnamic acid derivatives against human lung adenocarcinoma and colon carcinoma cells (Yen et al., 2011; Tsai et al., 2013; Ling et al., 2015).

Finally, the colony formation assay was performed (Franken et al., 2006) to investigate whether cinnamic acid derivative **9a** could influence the colony-formation of B16-F10 cells. The colony-forming activity of B16-F10 cells was suppressed after treatment with compound **9a** at 12.5 (25.5%), 25 (20.6%) and 50 (93.1%) $\mu\text{mol L}^{-1}$ (Fig. 6), with a reduction in the number of colonies when compared to vehicle-treated cells (0.4% DMSO).

Altogether, we may suggest that the compound **9a** was efficient in reducing metastatic potential of B16-F10 cells *in vitro*. The endpoints tested herein, including cell migration, proliferation, invasion, adhesion, and colonization, have been described as pivotal steps in the metastasis process *in vivo* (Kumar e Weaver, 2009; Guan, 2015). For instance, mouse models have been widely used for unraveling the complex interactions involved in the metastatic cascade, as well as for testing potential therapies against tumor cell migration (Gómez-Cuadrado et al. 2017). In this context, our findings could be considered a baseline for the study of the efficiency of cinnamic acid derivatives in animal model.

3.3. Effect of compound **9a** in non-tumor cell and erythrocyte viability

Herein, we evaluated the cytotoxicity of compound **9a** over non-tumoral cell lineages, as well as primary erythrocytes, since it has proved to be a promising antimetastatic agent. Vero and fibroblast (NIH3T3) cells were slightly sensitive to the compound **9a** at 100 $\mu\text{mol L}^{-1}$ (Fig. 7A). Moreover, there was no indicative of hemolysis for treatments with the derivative at different concentrations (Fig. 7B).

The slightly sensitivity of fibroblasts to the compound **9a** may also indicates that it is not a skin sensitizer (Tomankova et al., 2011). The *in silico* ADMET analysis, in addition, revealed that derivative **9a** has no ability to induce allergic contact dermatitis, and relatively low skin permeability (Table S2).

Moreover, this analysis showed that the most active derivative does not violate the Lipinsky's rules of five (Lipinsk, 2000), and therefore this compound is drug like. The prediction of absorption indicated that the compound **9a** has a high percentage of intestinal absorption, especially if orally administered. In the kidney, the compound **9a** is not an organic cation transporter 2 substrate, and it is potentially filtrated and partially reabsorbed in renal tubules. This result is important for determining dosing rates to

achieve steady-state concentrations. With respect to its toxicity, the compound **9a** is not a mutagenic compound and, therefore, may not act as a carcinogen. Although it is not a skin sensitizer, the compound **9a** may be associated with disrupted normal hepatic function (Table S2). The latter, in turn, can be verified in studies using animal models. Collectively, these findings indicate that compound **9a** seems to be non-toxic agent, enabling its application in more advanced *in vivo* studies.

3.4 Gelatin zymography and molecular docking help to understand the activity suppress of MMP -2 and -9 by compound 9a

It is well documented that MMP-9 and -2 are directly involved in melanoma progression (van den Oord et al., 1997; Hofmann et al., 2000; Kondratiev et al., 2008; Zhang et al., 2017). Both MMP enzymes are capable of degrading components from basement membranes. For that reason, they are probably related to the metastasis steps in melanoma (Hofmann et al., 2000; Gu et al., 2016). In this context, MMPs are important targets for the development of new drugs with antimetastatic activity. Cinnamic acid and its derivatives have demonstrated to be inhibitors of the MMPs activities (Yen et al., 2011; Tsai et al., 2013; Ling et al., 2015; Gopi et al., 2016). In the current study, B16-F10 cells were treated with compound **9a** for 24 h and analyzed by gelatin zymography in order to clarify whether the MMP-9 and -2 are related to the antimetastatic behavior of this compound. Our results showed that MMP-9 activity was suppressed after treatment with compound **9a** at 100 (64.26%) and 150 (63.85%) $\mu\text{mol L}^{-1}$ compared to vehicle-treated cells (0.4% DMSO; Fig. 8). Similarly, MMP-2 activity was suppressed by compound **9a** at 100 (48.75%) and 150 (43.90%) $\mu\text{mol L}^{-1}$ (Fig. 8). These findings are in accordance to previous reports revealing the cinnamic acid and its derivatives ability to inhibit the activities of MMP-9 and -2 in tumor cells, as well as

their capability of adhesion, migration, and invasion (Chiriac et al., 2005; Ali et al., 2014).

In order to shed light on the way that compound **9a** interacts with the aforementioned metalloproteinases, this compound, the cinnamic acid (Yen et al., 2011), and their derivatives that activity on MMP-9 and -2 have been previously described (Tsai et al., 2013) were anchored with human MMP-9 (PDB-ID: 1L6J) and -2 (PDB-ID: 1QIB). Those MMPs are directly involved in the progression of melanoma and indicates a poor prognosis (Hofmann et al., 2000; Gu et al., 2016). The anchorage investigation showed that compound **9a** displayed the best predicted binding affinity values for MMP-9 (-8.2 kcal / mol) and -2 (-8.6 kcal / mol) (Table 1).

The binding region of compound **9a** with MMP-9 (Fig. 9A) and -2 (Fig. 9C) is predicted to match to the active site, as well as observed for the cinnamic acid and their derivatives. As shown in Fig. 9B, the compound **9a** has potential to interact with catalytic aspartate residues Asp182 and Asp185 of MMP-9 with distance of 3.5 Å and 3.6 Å, respectively. The Fig. 9D showed that compound **9a** in the docking model interacts with catalytic glutamate residues, Glu150, Glu184 and Glu202 of MMP-2 with distance of 9.6 Å, 9.1 Å and 2.2 Å, respectively.

Our results revealed that compound **9a** is effective in inhibiting the metastatic behavior of B16-F10 melanoma cells. Furthermore, the prediction of molecular binding indicated that the inhibitory ability of this compound is mainly related to its interaction with MMP-9 and MMP-2. Similarly, previous studies have shown that cinnamic acid derivatives are potent inhibitors of MMPs (Zhang et al., 2006; Yen et al., 2011; Melo and Qsar, 2012; Tsai et al., 2013; Ling et al., 2015; Gopi et al., 2016). The reason for this inhibitory activity has been ascribed to the presence of heteroatoms (especially the hydroxyl group) in these compounds. The heteroatoms are capable of establishing hydrogen bonds with the proteins. In addition, the π electrons present in this compound

facilitate interactions with hydrophobic regions of the MMP-9 and -2 (Zhang et al., 2006; Yen et al., 2011; Melo and Qsar, 2012; Tsai et al., 2013; Ling et al., 2015; Gopi et al., 2016).

4. Conclusions

In the present study, twenty-six cinnamic acid derivatives containing 1,2,3-triazolic portions were synthesized and submitted to *in vitro* bioassays to investigate their activity over the metastatic behavior of murine melanoma. The most potent compound **9a**, a 1,2,3-triazolic-cinnamic acid derivative containing a benzyl group attached to the triazolic portion, presented significant antimetastatic activity against B16-F10 melanoma cells. The molecular docking simulation contributes to understanding our *in vitro* experimental results, demonstrating that compound **9a** has binding affinity with MMP-9 and -2. Therefore, our findings suggest that cinnamic acid derivatives containing a 1,2,3-triazolic portion may represent a scaffold to be explored towards the development of novel candidates for controlling malignant metastatic melanoma.

Acknowledgements

This work was supported by the Programa Nacional de Cooperação Acadêmica (PROCAD) of the Coordenação de Aperfeiçoamento de Pessoal de Nível Superior (CAPES), Conselho Nacional de Desenvolvimento Científico e Tecnológico (CNPq), and Fundação de Amparo à Pesquisa do Estado de Minas Gerais (FAPEMIG). The funders had no involvement in the study design, in the collection, analysis or interpretation of data, in the writing of the report, or in the decision to submit the article for publication. The authors also thank CNPq, FAPEMIG and CAPES for the fellowships to students and researchers involved in this work.

References

- Agaësse, G., Barbolat-Boutrand, L., El Kharbili, M., Berthier-Vergnes, O., Masse, I., 2017. p53 targets TSPAN8 to prevent invasion in melanoma cells. *Oncogenesis*. 6, e309.
- Ali, M., Abul Farah, M., Al-Hemaid, F., Abou-Tarboush, F., 2014. *In vitro* cytotoxicity screening of wild plant extracts from Saudi Arabia on human breast adenocarcinoma cells. *Genet. Mol. Res.* 13, 3981-3990.
- Anasamy, T., Thy, C.K., Lo, K.M., Chee, C.F., Yeap, S.K., Kamalidehghan, B., Chung, L.Y., 2017. Tribenzyltin carboxylates as anticancer drug candidates: Effect on the cytotoxicity, motility and invasiveness of breast cancer cell lines. *Eur. J. Med. Chem.* 125, 770-783.
- Astin, J.W., Batson, J., Kadir, S., Charlet, J., Persad, R.A., Gillatt, D., Oxley, J.D., Nobes, C.D., 2010. Competition amongst Eph receptors regulates contact inhibition of locomotion and invasiveness in prostate cancer cells. *Nat. Cell Biol.* 12, 1194-1204.
- Bhatia, S., Tykodi, S.S., Thompson, J.A., 2009. Treatment of metastatic melanoma: an overview. *Oncology (Williston Park, NY)*. 23, 488-496.
- Borgati, T.F., Alves, R.B., Teixeira, R.R., Freitas, R.P.d., Perdigão, T.G., Silva, S.F.d., Santos, A.A.d., Bastidas, A.d.J.O., 2013. Synthesis and phytotoxic activity of 1, 2, 3-triazole derivatives. *J. Braz. Chem. Soc.* 24, 953-961.
- Bradford, M.M., 1976. A rapid and sensitive method for the quantitation of microgram quantities of protein utilizing the principle of protein-dye binding. *Anal. Biochem.* 72, 248-254.
- Chen, H.-C., 2005. Boyden chamber assay, in: *Cell migration*, Springer, pp. 15-22.

- Chiriac, C., Tanasa, F., Onciu, M., 2005. A novel approach in cinnamic acid synthesis: direct synthesis of cinnamic acids from aromatic aldehydes and aliphatic carboxylic acids in the presence of boron tribromide. *Molecules*. 10, 481-487.
- Dias, D.A., Urban, S., Roessner, U., 2012. A historical overview of natural products in drug discovery. *Metabolites*. 2, 303-336.
- Elias, E.G., Hasskamp, J.H., Sharma, B.K., 2010. Biology of human cutaneous melanoma. *Cancers*. 2, 165-189.
- Franken, N.A., Rodermond, H.M., Stap, J., Haveman, J., Van Bree, C., 2006, Clonogenic assay of cells *in vitro*. *Nat. Protoc*. 1, 2315-2319.
- Gopi Krishna Reddy, A., Satyanarayana, G., 2016. Metal-free domino one-pot decarboxylative cyclization of cinnamic acid esters: Synthesis of functionalized indanes. *J. Org. Chem*. 81, 12212-12222.
- Gray-Schopfer, V., Wellbrock, C., Marais, R., 2007. Melanoma biology and new targeted therapy. *Nature*. 445, 851-857.
- Gu, L., Li, X., Ran, Q., Kang, C., Lee, C., Shen, J., 2016. Antimetastatic activity of novel ruthenium(III) pyridine complexes. *Cancer Med*. 5, 2850-2860.
- Guan, X., 2015. Cancer metastases: challenges and opportunities. *Acta Pharm. Sin. B*. 5, 402-418.
- Gullo, V.P., McAlpine, J., Lam, K.S., Baker, D., Petersen, F., 2006. Drug discovery from natural products. *J. Ind. Microbiol. Biotechnol*. 33, 523-531.
- Gómez-Cuadrado, L., Tracey, N., Ma, R., Qian, B., Brunton, V.G. 2017. Mouse models of metastasis: progress and prospects. *Dis Model Mech*. Sep 1; 10(9): 1061-1074.
- Hanahan, D., Weinberg, R.A., 2011. Hallmarks of cancer: the next generation. *Cell*. 144, 646-674.

- Harvey, A.L., 2008. Natural products in drug discovery. *Drug Discov. Today*. 13, 894-901.
- Hofmann, U.B., Westphal, J.R., van Muijen, G.N., Ruiter, D.J., 2000. Matrix metalloproteinases in human melanoma. *J. Invest. Dermatol.* 115, 337-344.
- Hulkower, K.I., Herber, R.L., 2011. Cell migration and invasion assays as tools for drug discovery. *Pharmaceutics*. 3, 107-124.
- Kondratiev, S., Gnepp, D.R., Yakirevich, E., Sabo, E., Annino, D.J., Rebeiz, E., Laver, N.V., 2008. Expression and prognostic role of MMP2, MMP9, MMP13, and MMP14 matrix metalloproteinases in sinonasal and oral malignant melanomas. *Hum. Pathol.* 39, 337-343.
- Kumar, S., Weaver, V.M., 2009. Mechanics, malignancy, and metastasis: the force journey of a tumor cell. *Cancer and Metastasis Rev.* 28, 113-127.
- Lam, K.S., 2007, New aspects of natural products in drug discovery. *Trends Microbiol.* 15, 279-289.
- Lee, H., Pyo, M.-J., Bae, S.K., Heo, Y., Kim, C.G., Kang, C., Kim, E., 2015. Improved therapeutic profiles of PLA2-free bee venom prepared by ultrafiltration method. *Toxicol. Res.* 31, 33-40.
- Liang, C.-C., Park, A.Y., Guan, J.-L., 2007. *In vitro* scratch assay: a convenient and inexpensive method for analysis of cell migration *in vitro*. *Nat. Protoc.* 2, 329.
- Ling, Y., Zhao, X., Li, X., Wang, X., Yang, Y., Wang, Z., Wang, X., Zhang, J., Zhang, Y., 2015. Novel FTS-diamine/cinnamic acid hybrids inhibit tumor cell proliferation and migration and promote apoptosis via blocking Ras-related signaling *in vitro*, *Cancer Chemother. Pharmacol.* 75, 381-392.
- Lipinski, C.A., 2000. Drug-like properties and the causes of poor solubility and poor permeability. *J. Pharm. Toxicol. Methods.* 44, 235-249.

- Mao, S.-W., Chen, H., Yu, L.-F., Lv, F., Xing, Y.-J., Liu, T., Xie, J., Tang, J., Yi, Z., Yang, F., 2016. Novel 3,4-seco bile acid diamides as selective anticancer proliferation and migration agents. *Eur. J. Med. Chem.* 122, 574-583.
- Melo, E.B.D., QSAR, A., 2012. Study of matrix metalloproteinases type 2 (MMP-2) inhibitors with cinnamoyl pyrrolidine derivatives. *Scientia Pharmaceutica.* 80, 265-282.
- Pietraszek, K., Brézillon, S., Perreau, C., Malicka-Błaszkiwicz, M., Maquart, F.-X., Wegrowski, Y., 2013. Lumican-derived peptides inhibit melanoma cell growth and migration. *PLoS one.* 8, e76232.
- Pires D.E., Blundell T.L., Ascher D.B., 2015. pkCSM: Predicting small-molecule pharmacokinetic and toxicity properties using graph-based signatures. *J. Med. Chem.* 2015, 14, 4066-72.
- Rodriguez L.G., Wu X., Guan J.L., (2005) Wound-Healing Assay. In: Guan JL. (eds) Cell Migration. *Methods in Molecular Biology™*, vol 294. Humana Press.
- Schmidt, B., Ribnicky, D.M., Poulev, A., Logendra, S., Cefalu, W.T., Raskin, I., 2008. A natural history of botanical therapeutics. *Metabolism.* 57, S3-S9.
- Sharma, A., Prasad, D., Singh, R.K., 2011. Journal of Chemical and Pharmaceutical Research. *J. Chem.* 3, 424-431.
- Shtivelman, E., Davies, M.A., Hwu, P., Yang, J., Lotem, M., Oren, M., Flaherty, K.T., Fisher, D.E., 2014. Pathways and therapeutic targets in melanoma. *Oncotarget.* 5, 1701-1752.
- Siegel, R.L., Miller, K.D., Jemal, A., 2015. Cancer statistics, 2015. *CA Cancer J. Clin.* 65, 5-29.

- Siqueira, R.P., Barbosa, É.d.A.A., Polêto, M.D., Righetto, G.L., Seraphim, T.V., Salgado, R.L., Ferreira, J.G., de Andrade Barros, M.V., de Oliveira, L.L., Laranjeira, A.B.A., 2015. Potential antileukemia effect and structural analyses of SRPK inhibition by N-(2-(piperidin-1-yl)-5-(trifluoromethyl) phenyl) isonicotinamide (SRPIN340). *PloS one*. 10, e0134882.
- Sova, M., Perdih, A., Kotnik, M., Kristan, K., Rižner, T.L., Solmajer, T., Gobec, S., 2006. Flavonoids and cinnamic acid esters as inhibitors of fungal 17 β -hydroxysteroid dehydrogenase: A synthesis, QSAR and modelling study. *Bioorganic Med. Chem.* 14, 7404-7418.
- Tomankova K., Kejllova K., Binder S., Daskova A., Zapletalova J., Bendova H., Kolarova H., Jirova D., 2011. *In vitro* cytotoxicity and phototoxicity study of cosmetics colorants. *Toxicol. In Vitro.* 25, 1242-50.
- Trott, O., Olson, A.J., 2010. AutoDock Vina: improving the speed and accuracy of docking with a new scoring function, efficient optimization, and multithreading. *J. Comput. Chem.* 31, 455-461.
- Tsai, C.-M., Yen, G.-C., Sun, F.-M., Yang, S.-F., Weng, C.-J., 2013. Assessment of the anti-invasion potential and mechanism of select cinnamic acid derivatives on human lung adenocarcinoma cells. *Mol. Pharm.* 10, 1890-1900.
- van den Oord, J.J., Paemen, L., Opdenakker, G., Wolf-Peeters, C. de, 1997. Expression of gelatinase B and the extracellular matrix metalloproteinase inducer EMMPRIN in benign and malignant pigment cell lesions of the skin. *Am. J. Pathol.* 151, 665-670.
- Xu, T., Chi, B., Gao, J., Chu, M., Fan, W., Yi, M., Xu, H., Mao, C., 2017. Novel electrochemical immune sensor based on Hep-PGA-PPy nanoparticles for detection of α -Fetoprotein in whole blood. *Anal. Chim. Acta.* 977, 36-43.

Yen, G.-C., Chen, Y.-L., Sun, F.-M., Chiang, Y.-L., Lu, S.-H., Weng, C.-J., 2011. A comparative study on the effectiveness of cis-and trans-form of cinnamic acid treatments for inhibiting invasive activity of human lung adenocarcinoma cells. *Eur. J. Pharm. Sci.* 44, 281-287.

Zhang, L., Zhang, J., Fang, H., Wang, Q., Xu, W., 2006. Design, synthesis and preliminary evaluation of new cinnamoyl pyrrolidine derivatives as potent gelatinase inhibitors. *Bioorganic Med. Chem.* 14, 8286-8294.

Zhang, T., Suryawanshi, Y.R., Szymczyna, B.R., Essani, K., 2017. Neutralization of matrix metalloproteinase-9 potentially enhances oncolytic efficacy of tanapox virus for melanoma therapy. *Med. Oncol.* 34, 129.

Figure captions:

Fig. 1. Structures of cinnamic acid and some derivatives.

Fig. 2. Synthesis of esters **5** and **6**, and azides **7**. Reagents and conditions: (i) DCC, DMAP (10 mol%), CH₂Cl₂, r.t.; (ii) Et₃N, CH₃SO₂-Cl, CH₂Cl₂, -50 °C; (iii) NaN₃, DMSO, r.t.

Fig. 3. Reagents and conditions: (iv) sodium ascorbate (40 mol%), CuSO₄·5H₂O (20 mol%), CH₂Cl₂/H₂O (1:1 v/v), r.t.

Fig. 4. Effect of cinnamic acid derivatives containing 1,2,3-triazolic portions on wound healing and proliferation of B16-F10 melanoma cells *in vitro*. (A and B) B16-F10 cells were wounded with a pipette tip and then treated with 100 μmol L⁻¹ of each synthesized compound for 24 h. (C) B16-F10 cells were wounded and treated for

24 h with $50 \mu\text{mol L}^{-1}$ of the most active compounds as determined in (A and B). (D) Photos of the wound were taken at 0 and 24 h after treatment with $50 \mu\text{mol L}^{-1}$ of compound **9a** under 100 x magnitude microscope. (E) Chemical structure of compound **9a**. (F) Trypan blue dye exclusion assay of compound **9a** on the proliferation of B16-F10 cells. Mean \pm S.E.M. * $p < 0.05$, ** $p < 0.01$, *** $p < 0.001$ ou # $p < 0.0001$ versus control (0.4% DMSO) by Dunnett's test.

Fig. 5. Effect of compound 9a on invasion and adhesion of B16-F10 melanoma cells *in vitro*. (A) Photomicrography represents the cells invasion through matrigel coating (100 x magnification). (B) The bar graphs represent invasive cell number that was treated with 12.5, 25 and $50 \mu\text{mol L}^{-1}$ of compound **9a** for 24 h. (C) The bar graph represents the adhered cell number that was treated with 12.5, 25, and $50 \mu\text{mol L}^{-1}$ of compound **9a** for 12 h. Mean \pm S.E.M. * $p < 0.05$, ** $p < 0.01$ or *** $p < 0.001$ versus control (0.4% DMSO) by Dunnett's test.

Fig. 6. Effect of compound 9a on colony formation of B16-F10 melanoma cells *in vitro*. Photomicrography showing the formation of B16-F10 colonies after treatment with 12.5, 25 and $50 \mu\text{mol L}^{-1}$ of compound **9a** for 14 days. After that, the colonies were fixed with methanol, stained with toluidine blue solution and counted. Bar graphs represent the colony number that were formed after 14 d of treatment with compound **9a** at 12.5, 25 and $50 \mu\text{mol L}^{-1}$. Mean \pm S.E.M. * $p < 0.05$, ** $p < 0.01$ or *** $p < 0.001$ versus control (0.4% DMSO) by Dunnett's test.

Fig. 7. Cytotoxic effects of compound 9a on non-neoplastic cell lines and erythrocytes viability. (A) Vero (African green monkey kidney cell) and NIH3T3 (Embryonic fibroblasts) cells were exposed to $100 \mu\text{mol L}^{-1}$ compound **9a** for 48 h. (B)

Graphical of hemolysis assay. Mean \pm S.E.M. $**p < 0.01$ versus control (0.4% DMSO), and $\#p < 0.0001$ versus control (Triton) by Dunnett's test.

Fig. 8. Representative gelatin zymogram showing the effects of compound 9a on matrix metalloproteinase (MMP)-9 and -2 activities in treated B16-F10 melanoma cells. Cells were incubated with 0 (Control), 50, 100 and 150 $\mu\text{mol L}^{-1}$ of compound 9a for 24 h. The density of each band was quantified by densitometric analysis. Fetal bovine serum was used as weight standard (WE). M: medium. Mean \pm S.E.M. $*p < 0.01$ versus control (0.4% DMSO) by Dunnett's test.

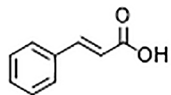
Fig. 9. Molecular interactions of compound 9a, cinnamic acid, and its derivatives with the active site (orange) of matrix metalloproteinases (MMP)-9 and -2. (A) Docking of compound 9a (blue), cinnamic acid (green), ferulic acid (red), chlorogenic acid (magenta), caffeic acid (yellow) with MMP-9. (B) Docking view showing compound 9a bond interaction of ligands with residues in the active site of MMP-9. Important residues Asp182 and Asp185 (green) of MMP-9 interaction between compound 9a (blue). (C) Docking of compound 9a (blue), cinnamic acid (green), ferulic acid (red), chlorogenic acid (magenta), caffeic acid (yellow) with MMP-2. (D) Docking view showing the compound 9a bond interaction of ligands with residues in the active site of MMP-2. Important residues Glu 150, Glu184 and Glu202 (green) of MMP2 interaction between compound 9a (blue). Zinc ion indicated in yellow (B, D).

Table 1. Predicted binding affinities of compound **9a**, cinnamic acid, ferulic acid, chlorogenic acid, and caffeic acid to matrix metalloproteinase (MMP)-9 and -2 by Autodock Vina program.

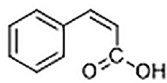
| Compounds | MMP-9 (PDB-ID:1L6J) | MMP-2 (PDB-ID:1QIB) |
|-----------------|------------------------|------------------------|
| | Bond energy (kcal/mol) | Bond energy (kcal/mol) |
| 9a | -8.2 | -8.6 |
| Cinnamic acid | -6.7 | -6.5 |
| Ferulic acid | -6.2 | -6.9 |
| Chorogenic acid | -6.8 | -6.5 |
| Caffeic acid | -5.8 | -7.6 |

Highlights

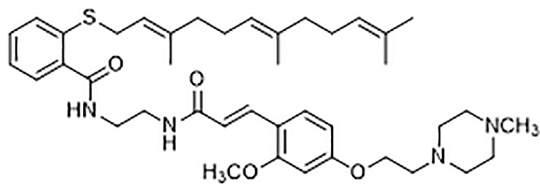
- Twenty six 1,2,3-triazole cinnamic acid derivatives were synthesized
- The antimetastatic activity of derivatives on B16F10 cell line was assessed
- 3-(1-benzyl-*1H*-1,2,3-triazol-4-yl)propyl cinnamate (**9a**) was the most active one
- The antimetastatic effect of **9a** seems to be linked with inhibition of MMP-9 and -2
- Docking studies revealed interactions of **9a** with the active site of MMP-9 and -2



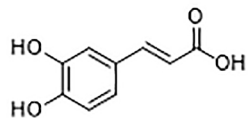
trans-Cinnamic acid



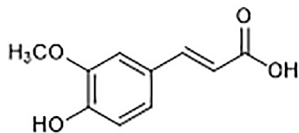
cis-Cinnamic acid



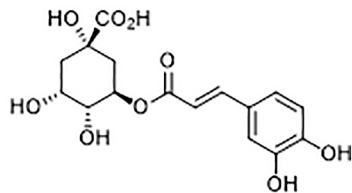
FTS-diamine/cinnamic acid hybrid
(1)



Caffeic acid
(2)

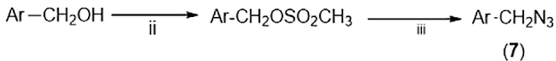
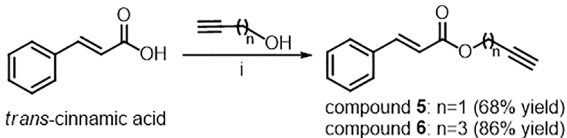


Ferulic acid
(3)



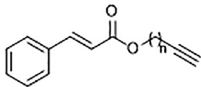
Chlorogenic acid
(4)

Figure 1

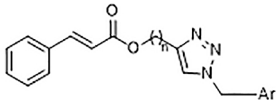
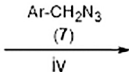


Ar = phenyl; 2,5-dichlorophenyl; 4-iodophenyl; 4-nitrophenyl; 4-bromophenyl;
 4-chlorophenyl; 3,4-difluorophenyl; 4-fluorophenyl; 4-trifluoromethoxyphenyl;
 4-trifluoromethylphenyl; 4-methoxyphenyl; 2,4,6-trichlorophenyl; 2-bromophenyl;
 2-fluorophenyl

Figure 2



compound 5: $n=1$
compound 6: $n=3$



8a-8m
9a-9m

Figure 3

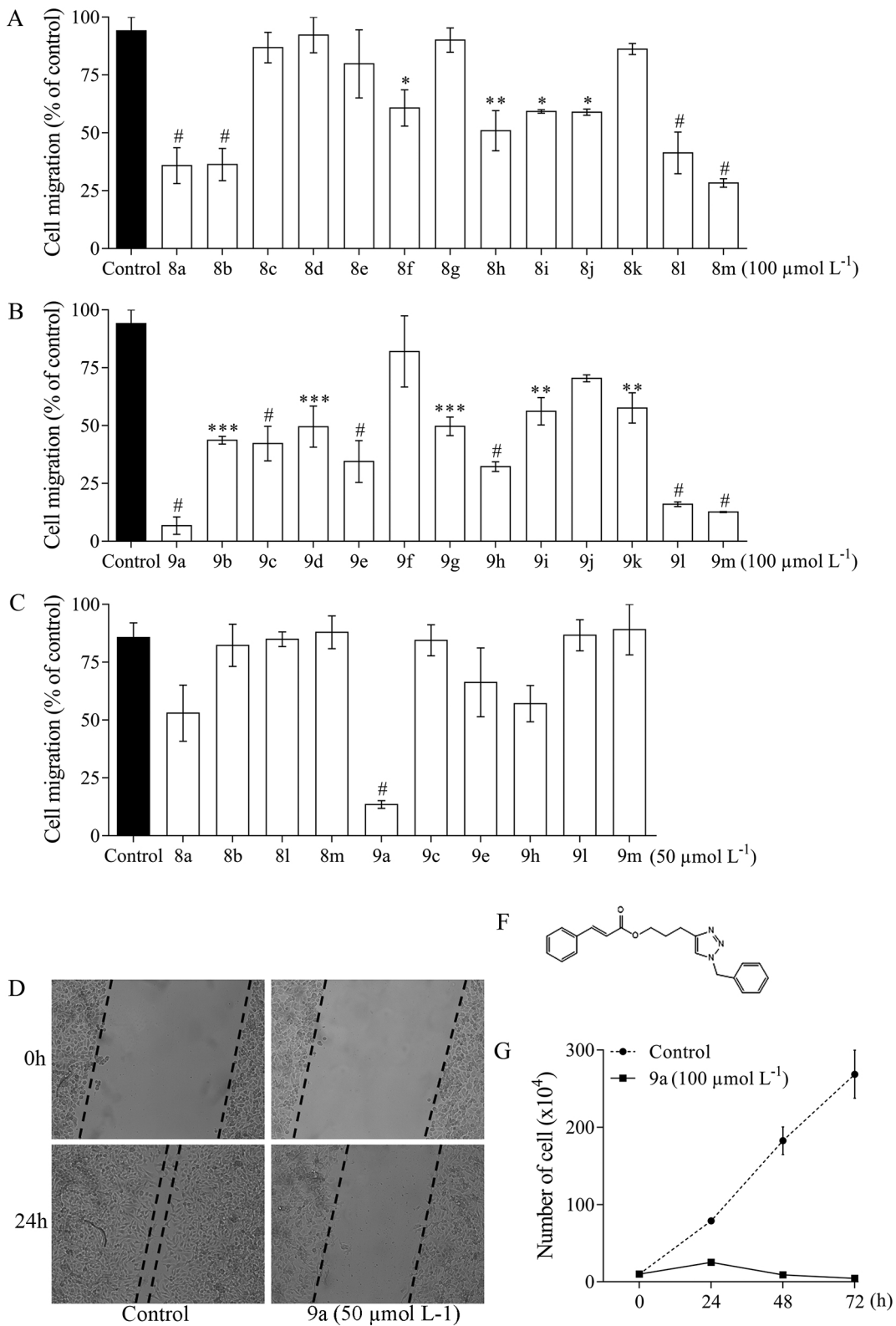


Figure 4

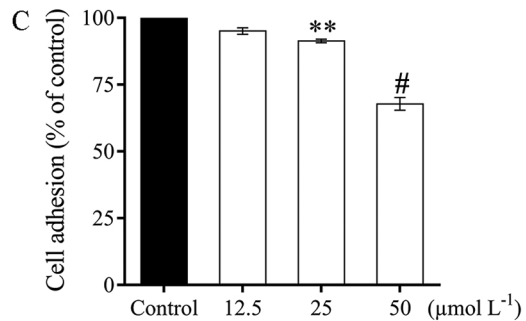
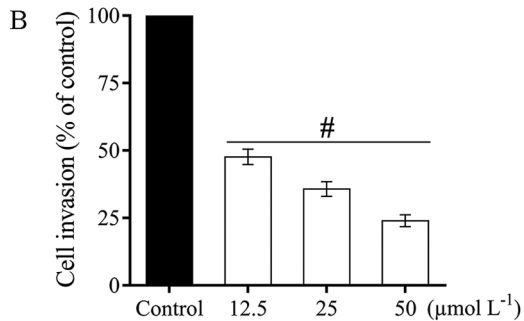
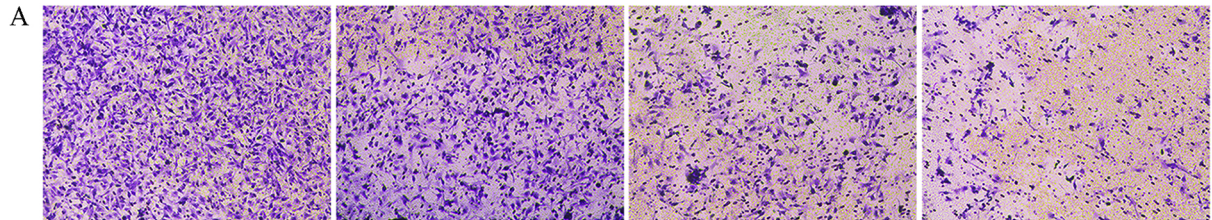


Figure 5

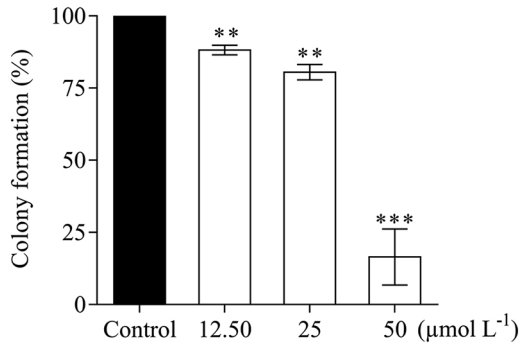
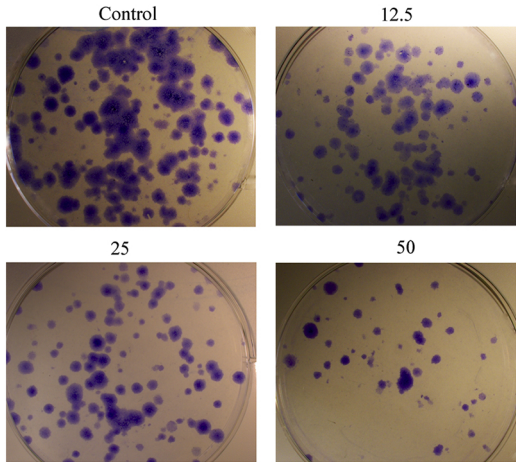


Figure 6

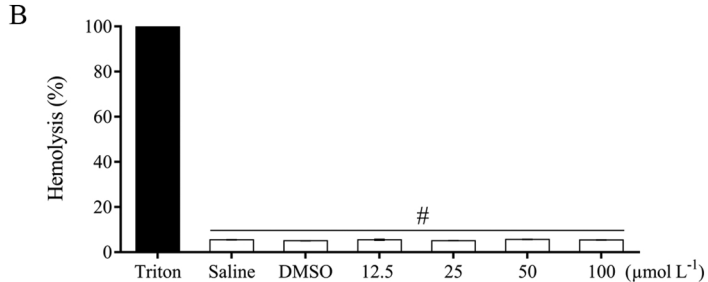
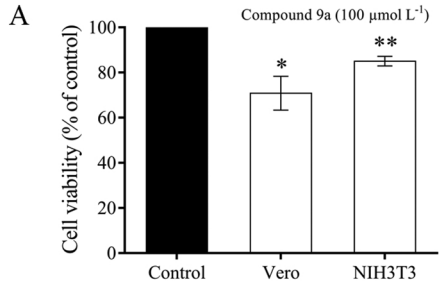


Figure 7

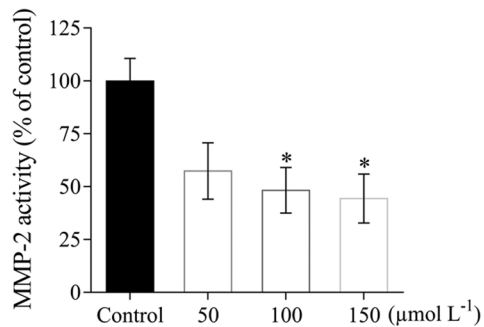
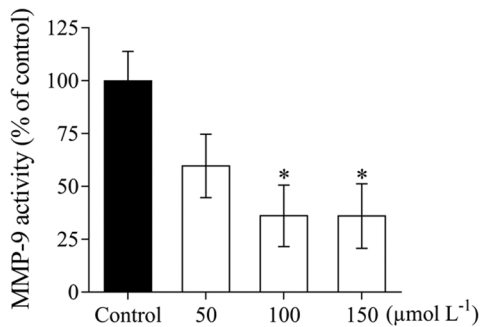
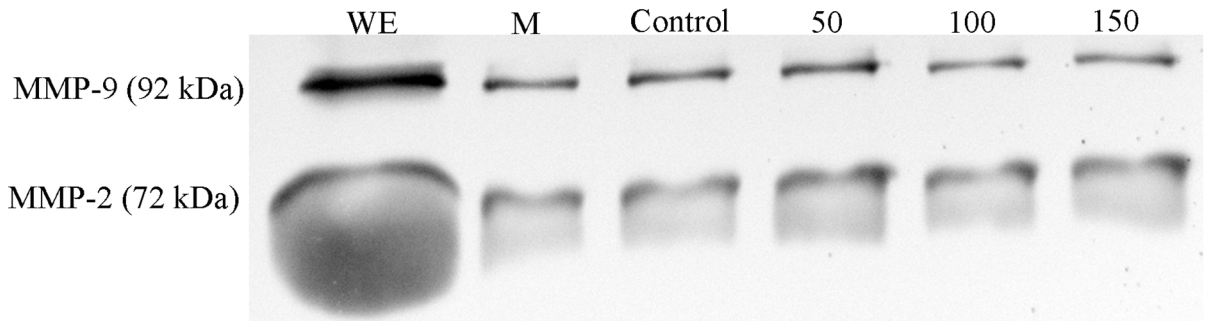
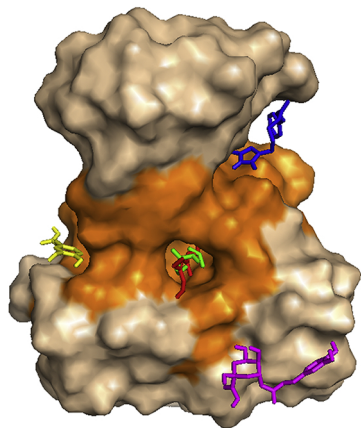
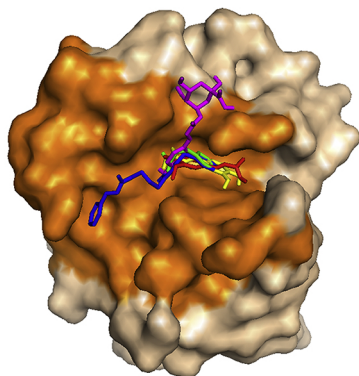


Figure 8

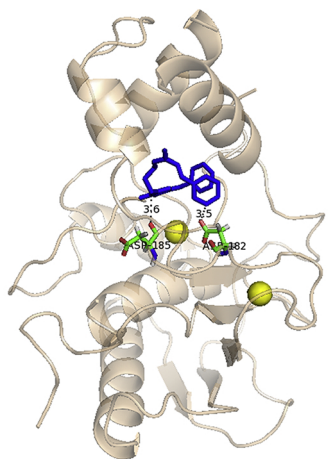
A



C



B



D

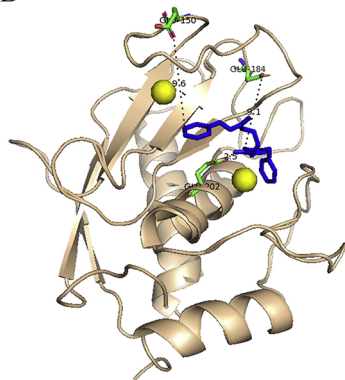


Figure 9